Electronic supplementary information

A post-reduction strategy to enhance near-infrared-II emission from Li$_4$SrCa(SiO$_4$)$_2$:Cr^{4+} phosphors

Yixin Sun,[a] Yining Wang,[a] Minliang Deng,[a] Xiaole Xing,[a] Yiying Zhu,[a] and Mengmeng Shang,*[a]

[a] Key Laboratory for Liquid-Solid Structural Evolution and Processing of Materials Ministry of Education, School of Material Science and Engineering, Shandong University, 17923 Jingshi Road, Jinan 250061, P. R. China. E-mail: mmshang@sdu.edu.cn

Table S1 Main parameters of processing and refinement results of LSCS:0.1%Cr^{4+} and LSCS:3%Cr^{4+}.

Compound	LSCS:0.1%Cr^{4+}	LSCS:3%Cr^{4+}
a, Å	4.9757	4.9757
b, Å	9.9216	9.9235
c, Å	14.0403	14.0395
V, Å^3	693.13	693.22
α, °	90	90
β, °	90	90
γ, °	90	90
R_{wp}, %	10.51	11.21
R_p, %	7.81	8.03
χ^2	3.032	3.222

Table S2 Luminescence properties of Cr^{4+}-doped Si-based NIR luminescent materials.

Materials	λ_{ex}, λ_{em} (nm)	Emission Range (nm)	FWHM (nm)	IQE	Ref.
Zn$_2$SiO$_4$:Cr^{4+}	800, 1350	1100 - 1600	300	1.7%	[S1]
Mg$_2$SiO$_4$:Cr^{4+}	800, 1130	800 - 1500	220	2.0%	[S1]
Li$_2$ZnSiO$_4$:Cr^{4+}	800, 1170	1000 - 1600	240	17%	[S1]
Li$_2$MgSiO$_4$:Cr^{4+}	800, 1210	1000 - 1500	230	2.2%	[S1]
Li$_2$CaSiO$_4$:Cr^{4+}	680, 1150	1000 - 1500	~ 200	--	[S2]
LSCS:Cr^{4+}	**465, 1215**	**900 - 1600**	**233**	**2.2%**	**This work**
LSCSH:Cr^{4+}	**465, 1215**	**900 - 1600**	**228**	**27%**	**This work**

Table S3 Main parameters of processing and refinement results of LSCSH:0.1%Cr^{4+} and LSCSH:3%Cr^{4+}.

Compound	LSCSH:0.1%Cr^{4+}	LSCSH:3%Cr^{4+}
a, Å	4.9778	4.9776
b, Å	9.9255	9.9255
c, Å	14.0464	14.0475
V, Å^3	693.99	694.02
α, °	90	90
β, °	90	90
γ, °	90	90
R_{wp}, %	10.84	12.08
R_p, %	7.95	8.78
χ^2	2.701	3.612

Table S4 Temperature sensing performance of various materials based on spectral shift ($\Delta\lambda$) and decay times (τ).
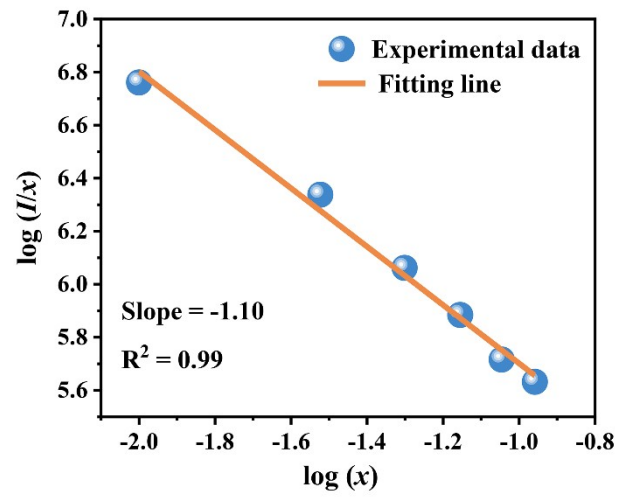
| Materials	Method	Maximum S_R (K^{-1})	Ref.
$Ca_2Al_2SiO_7$:Cr^{4+}	$\Delta\lambda$	0.61%	[S3]
	τ	0.25%	
$CaYGaO_4$:Cr^{4+}	$\Delta\lambda$	5.82% @100 K	[S4]
	τ	0.78% @350 K	
$Sr_4Al_{14}O_{25}$:Mn^{4+}	τ	1.5% @ 420 K	[S5]
CaZnOS:Mn^{2+}	τ	1.71% @ 150 K	[S6]
$Ba_3(VO_4)_2$:Mn^{4+}, Er^{3+}	τ	1.71% @ 150 K	[S7]
$Li_4SrCa(SiO_4)_2$:Cr^{4+}	**$\Delta\lambda$**	**1.71% @ 150 K**	**This**
	τ	**1.69% @ 425 K**	**work**
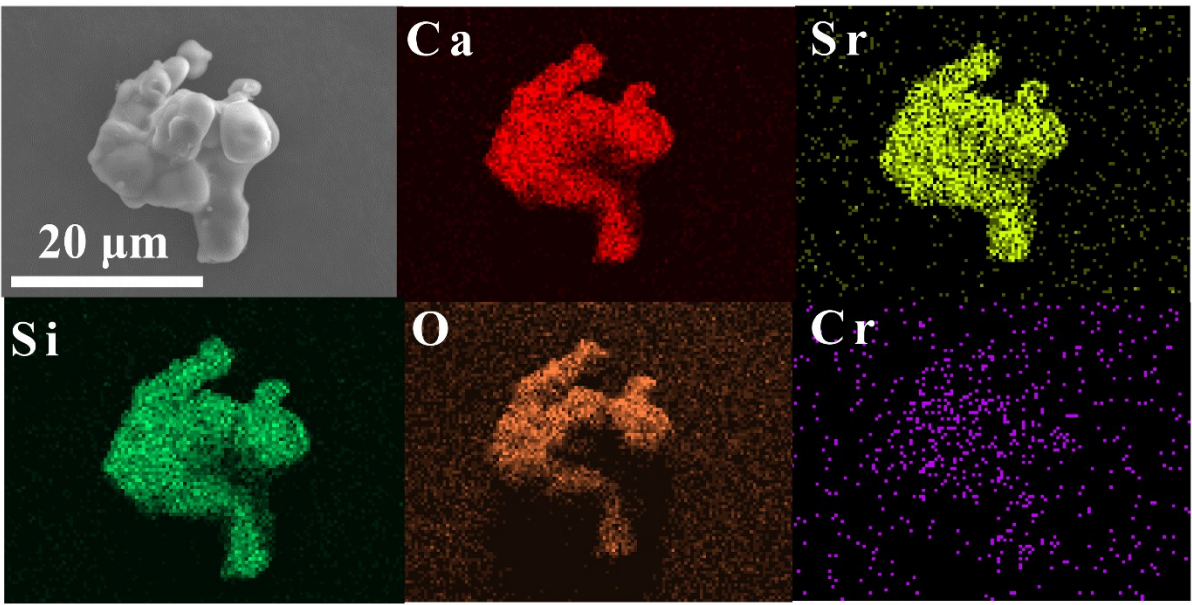
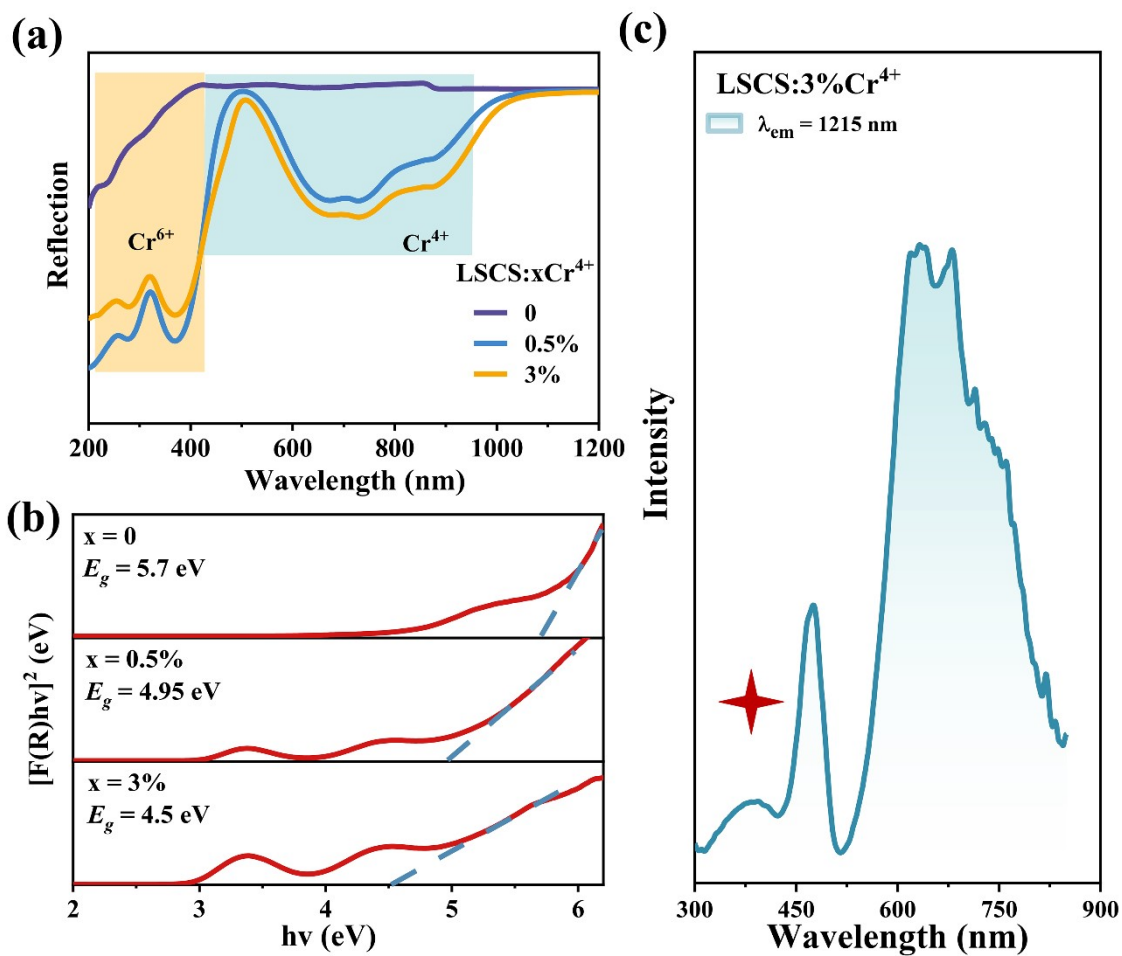**Fig. S1** SEM image and elemental mapping images of LSCS:3%Cr^{4+}.
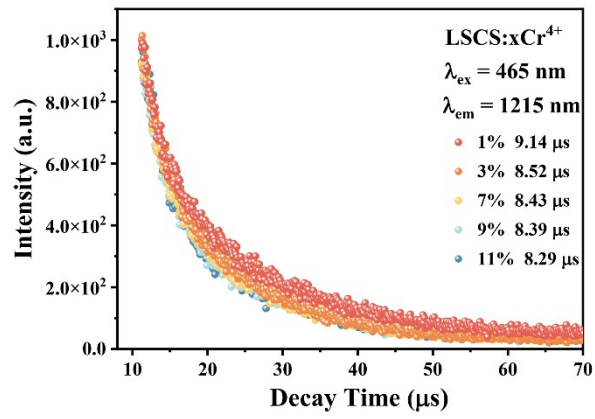
Fig. S2 Fluorescence decay curves of LSCS:xCr^{4+} (x = 1% ~ 11%).

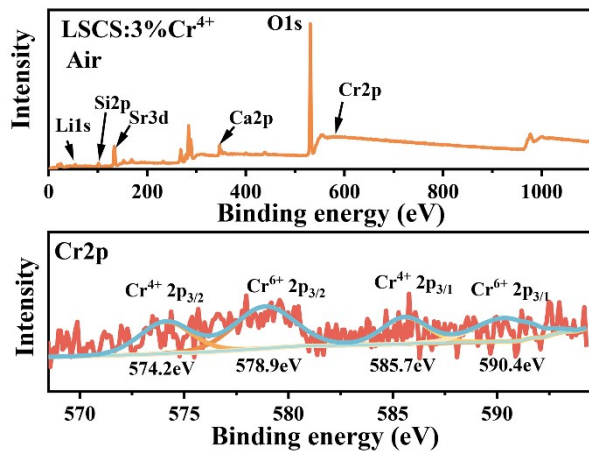**Fig. S3** The linear fitting of log (I/x) versus log (x) of LSCS:xCr^{4+} (x = 1% ~ 11%).
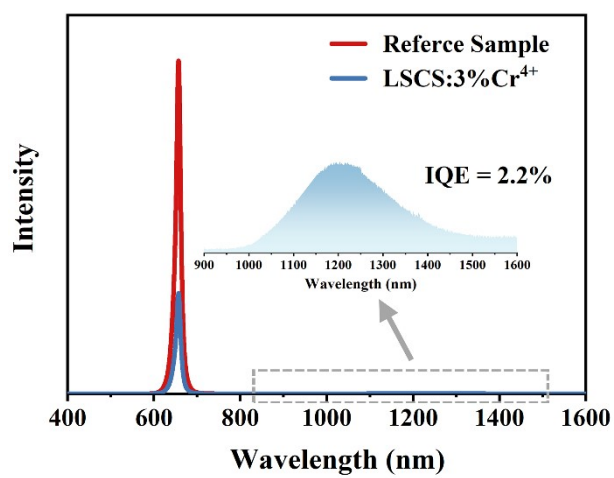
Fig. S4 The quantum efficiency of LSCS:3%Cr^{4+}.
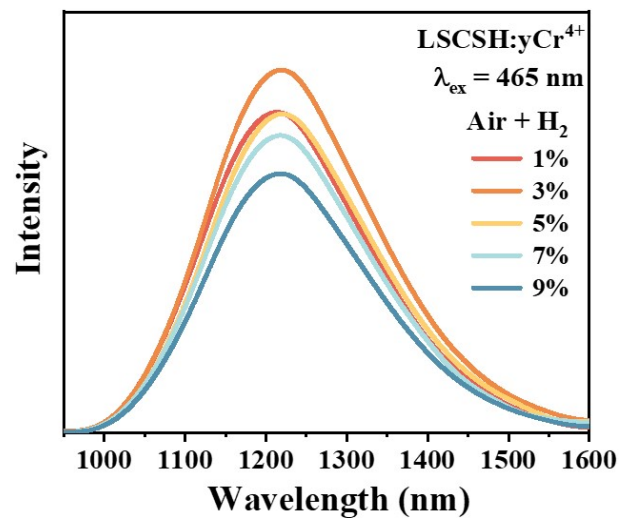
Fig. S5 (a) UV-vis-NIR DR spectra and (b) the optical band gap of LSCS:xCr^{4+} (x = 0, 0.5% and 3%). (c) The PLE spectrum of the LSCS:3%Cr^{4+}.
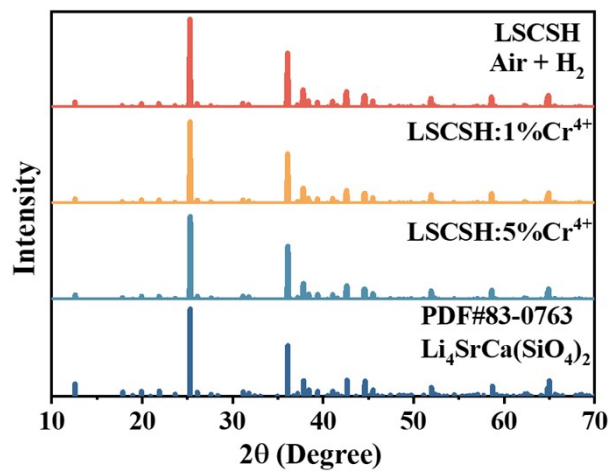
Fig. S6 The XPS survey spectrum and high-resolution XPS spectrum of Cr2p level of LSCS:3%Cr^{4+}.

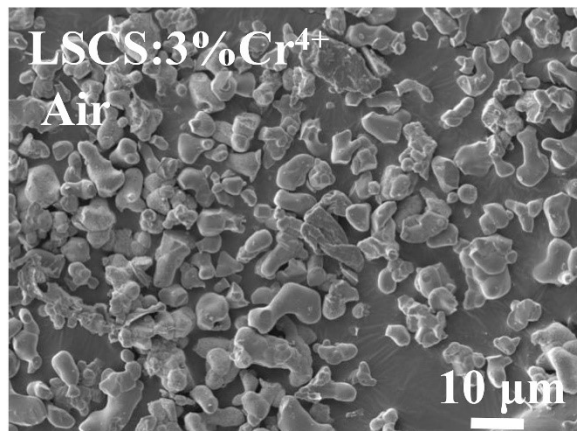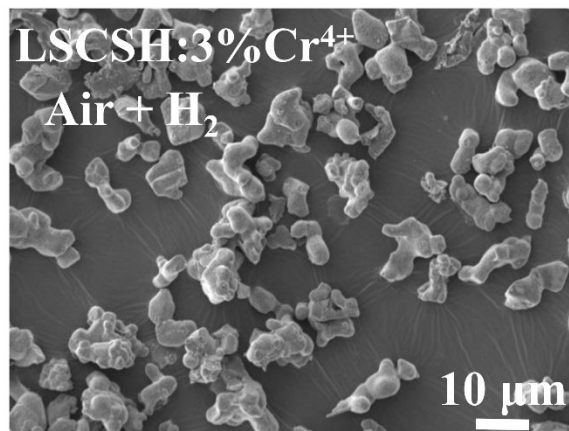**Fig. S7** The PL spectra of LSCSH:yCr^{4+}.

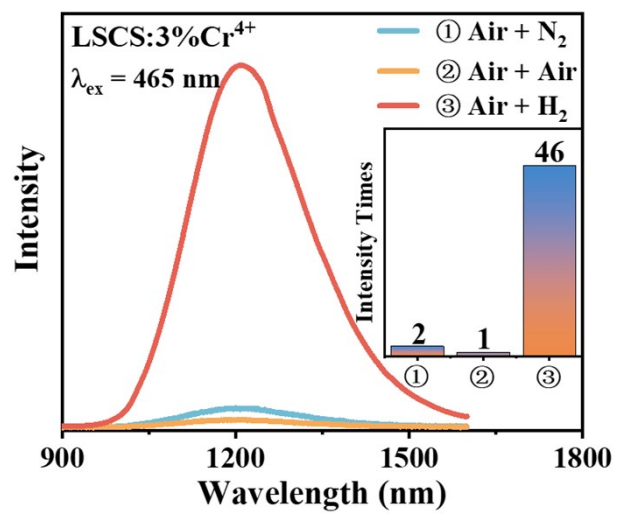**Fig. S8** XRD patterns of LSCSH:yCr^{4+} (y = 0, 1% and 5%).

(a)

LSCS:3%Cr^{4+}
Air

10 μm
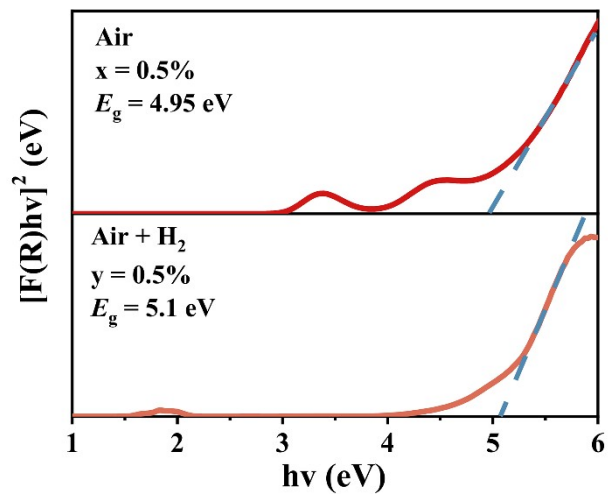
(b)

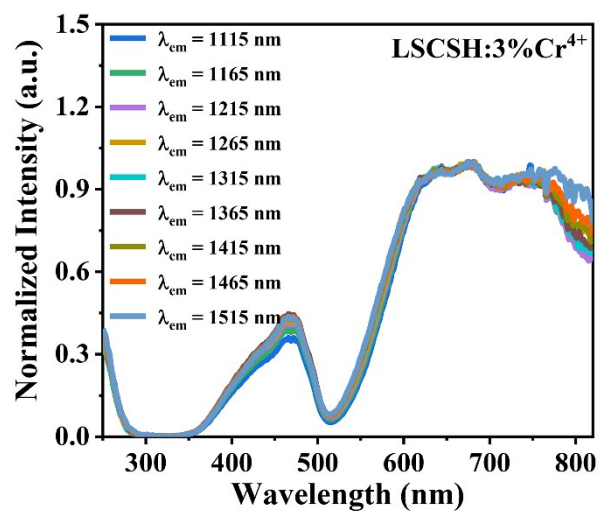LSCSH:3%Cr^{4+}
Air + H$_2$

10 μm

Fig. S9 SEM images of (a) LSCS:3%Cr^{4+} and (b) LSCSH:3%Cr^{4+}.
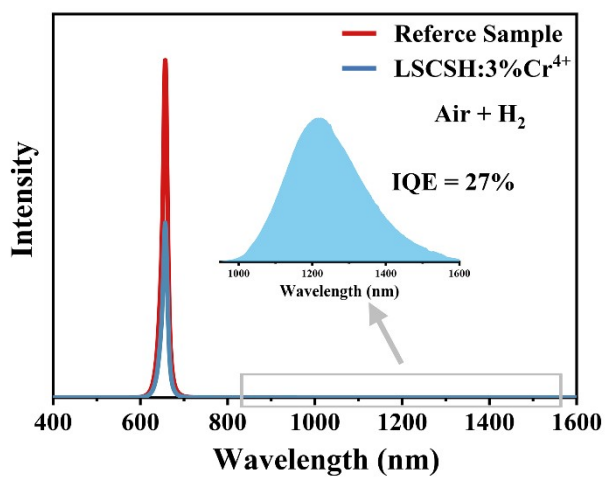
Fig. S10 The emission spectra of LSCS:3%Cr^{4+} under different sintering conditions.

Fig. S11 The optical band gap of LSCS:0.5%Cr^{4+} and LSCSH:0.5%Cr^{4+}.

Fig. S12 Monitoring normalized PLE spectra at 1115 - 1515 nm of LSCSH:3%Cr^{4+}.

Fig. S13 The quantum efficiency of LSCSH:3%Cr^{4+}.
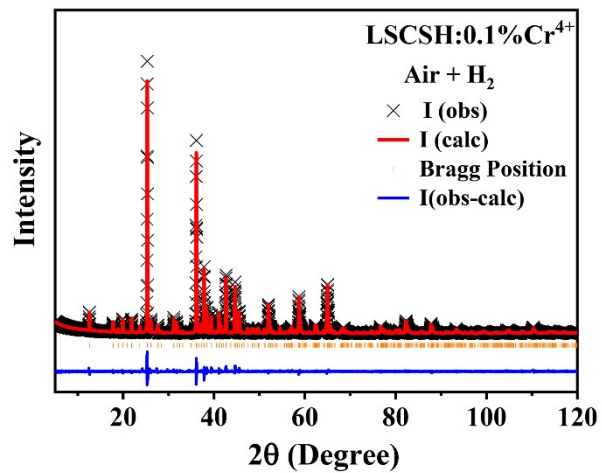
Fig. S14 The Rietveld refinement of LSCSH:0.1%Cr^{4+}.
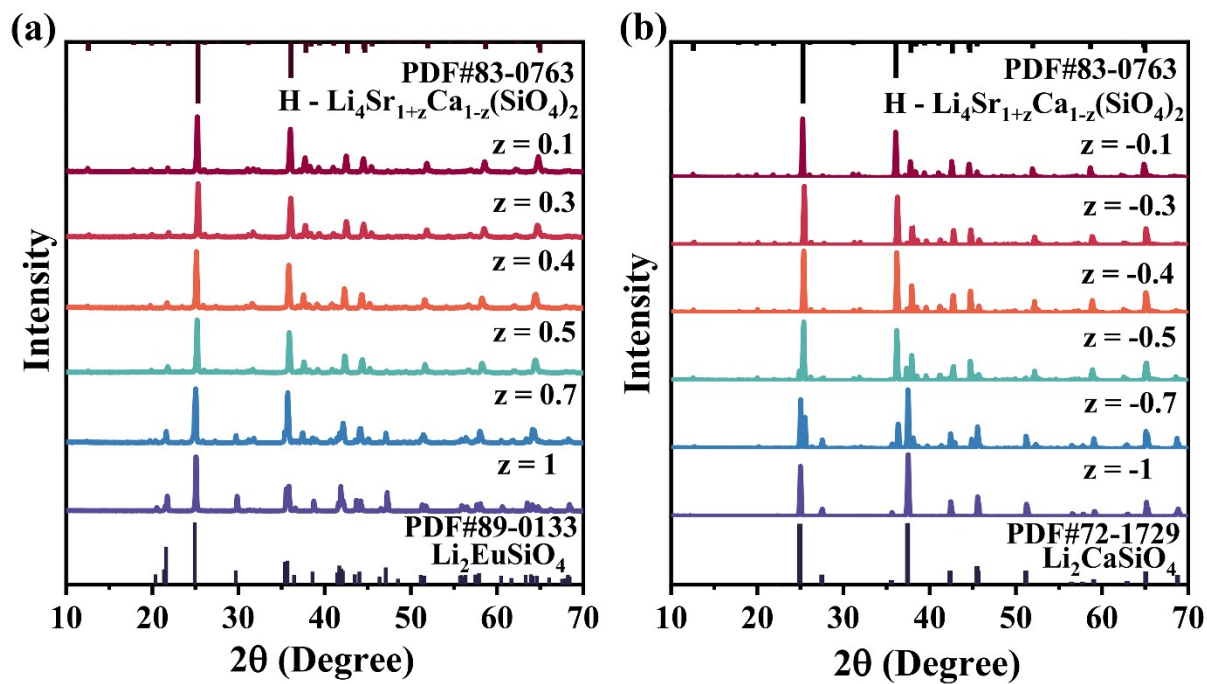
Fig. S15 XRD patterns of the H - $Li_4Sr_{1+z}Ca_{1-z}(SiO_4)_2$:3%$Cr^{4+}$ (a) z = 0.1 ~ 1 and (b) z = -1 ~ -0.1.
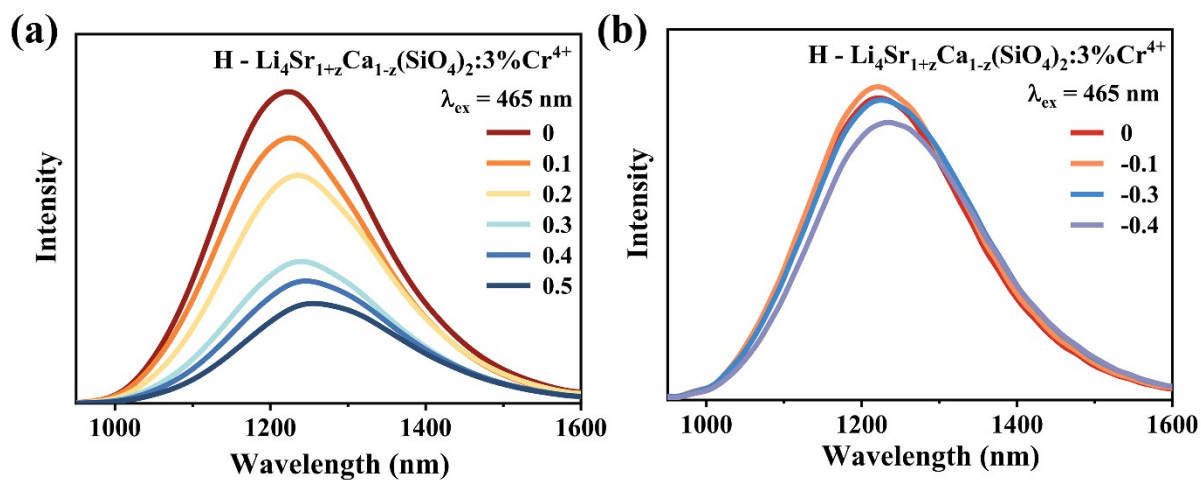
Fig. S16 The PL spectra of H - $Li_4Sr_{1+z}Ca_{1-z}(SiO_4)_2$:3%$Cr^{4+}$ (a) z = 0 ~ 0.5 and (b) z = -0.4 ~ 0.
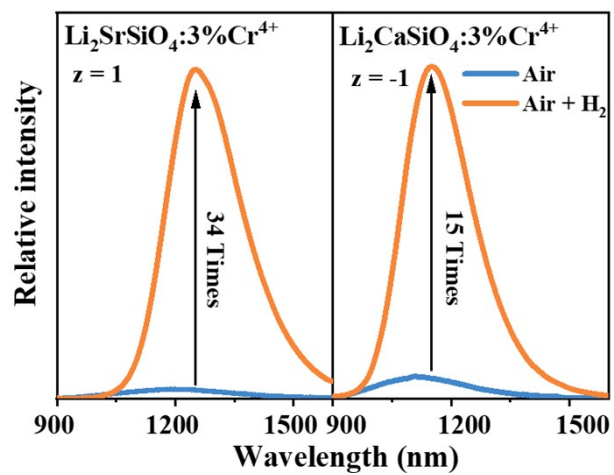
Fig. S17 The PL spectral intensity increased times of Li_2SrSiO_4:3%Cr^{4+} and Li_2CaSiO_4:3%Cr^{4+} by post-reduction strategy.
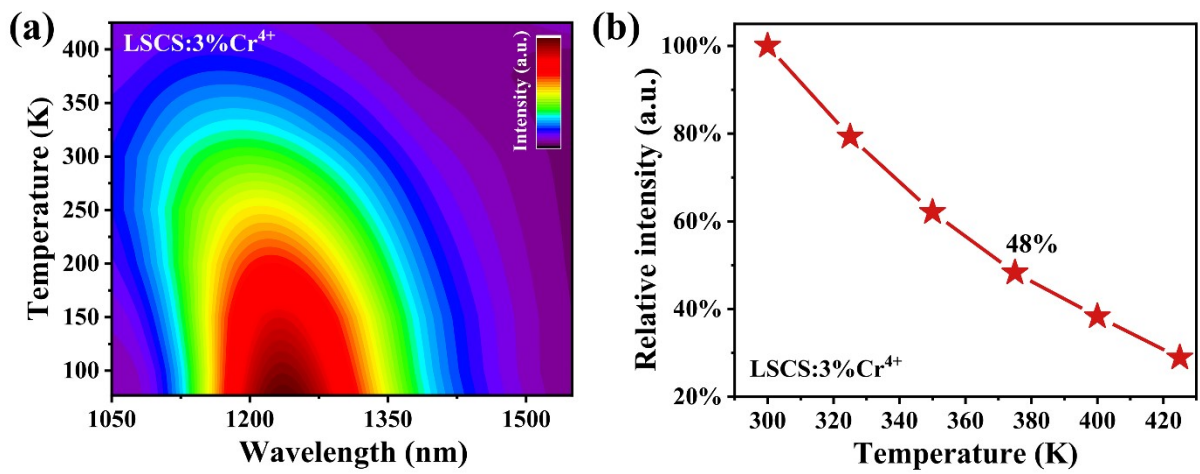
Fig. S18 Temperature-dependent (a) PL spectra and (b) relative emission intensity of LSCS:3%Cr^{4+}.
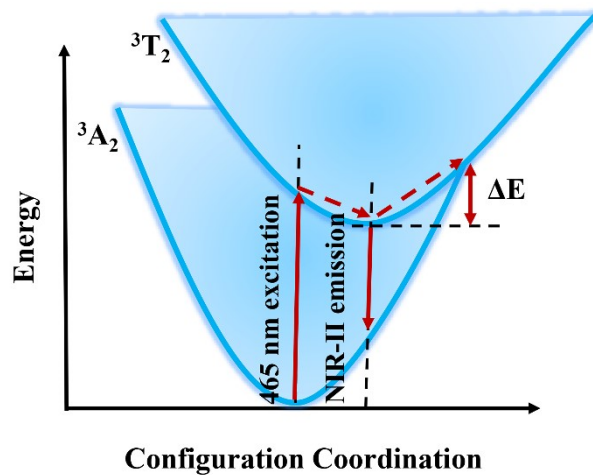
Fig. S19 Configurational coordinate diagram illustrating band broadening and thermal quenching behaviors of LSCSH:yCr^{4+}.
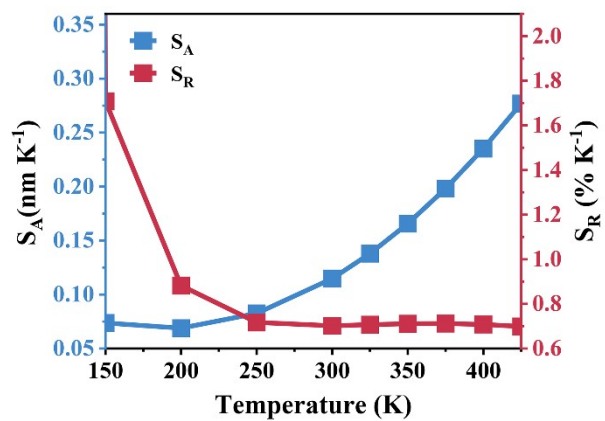
Fig. S20 Calculated S_A and S_R values via $\Delta\lambda$ changing with temperature.

To insight into the the nature of ion - ion interaction in the lattice, the critical distance R_c can be computed using the following formula:[S8]

$$R_c \approx 2 \left(\frac{3V}{4\pi X_c N} \right)^{\frac{1}{3}} \qquad (S1)$$

Within this equation, V represents the unit cell volume, X_c stands for the critical concentration and N signifies the number of sites within a unit cell where Cr^{4+} ions can substitute. In this scenario, $V = 693.22$ $Å^3$, $N = 4$ and $X_c = 0.03$. The computed value for R_c is 22.26 Å, significantly exceeding the critical distance of 5 Å for exchange interaction. Therefore, the non-radiative energy transfer mechanism is multipolar interaction. The type of interaction between Cr ions is calculated by eqn. S2:[S9]

$$\frac{I}{x} = K \left[1 + \beta(x)^{\frac{\theta}{3}} \right]^{-1} \qquad (S2)$$

Where I represents for the PL spectra intensity and x stands for the corresponding activator concentration, K and β are constants. Fig. S3 depicts the linear fitting of log (I/x) to log (x), yielding a slope of -1.10 and θ as 3.30. This indicates that the energy transfer between neighboring ions serves as the main concentration quenching mechanism of LSCS:xCr^{4+}, since θ is close to 3.

The optical band gap can be calculated using the following Kubelka-Munk formula:[S10,S11]

$$F(R) = \frac{(1-R)^2}{2R} \tag{S3}$$

$$[F(R) \times hv]^{1/n} = A(hv - E_g) \tag{S4}$$

where $F(R)$ is the absorption, R is the reflectance, hv is the photon energy, A is the absorption constant, and E_g is the optical band gap. The n values determined by the directly allowed transition, directly forbidden transition, indirectly allowed transition, and indirectly forbidden transition are 1/2, 3/2, 2, and 3, respectively. The electronic transition of this garnet belongs to directly allowed transition ($n = 1/2$), so the E_g is estimated to be 5.7 eV (LSCS), 4.95 eV (LSCS:0.5%Cr^{4+}), 4.5 eV (LSCS:3%Cr^{4+}) and 5.1 eV (LSCSH:0.5%Cr^{4+}) respectively.

The activation energy (ΔE) can further evaluate thermal stability and can be computed using the Arrhenius formula:[S12-S14]

$$I_T = \frac{I_0}{1 + Aexp(\dfrac{-\Delta E}{kT})} \qquad (S5)$$

Where, I_T is the luminous intensity at temperature T, I_0 is the original intensity, A is a constant, and k is 8.617×10^{-5} eV K^{-1} (Boltzmann constant). The calculated $\Delta E = 0.19$ eV for LSCSH:3%Cr^{4+}.

References

[S1] Y. Zhuang, S. Tanabe, J. Qiu, *J. Am. Ceram. Soc.*, 2014, **97**, 3519-3523.

[S2] M. Y. Sharonov, A. B. Bykov, V. Petričević, R. R. Alfano, *Opt. Commun.*, 2004, **231**, 273.

[S3] X.Chen, S.Liu, K.Huang, J.Nie, R.Kang, X.Tian, S.Zhang, Y.Li, J. Qiu, *Chem. Eng. J.*, 2020, **396**, 125201.

[S4] Y. Wang, G. Liu, Z. Xia, *Laser Photon. Rev.*, 2023, 2300717.

[S5] M. Pieprz, W. Piotrowski, P. Woźny, M. Runowski, L. Marciniak, *Adv. Opt. Mater.*, 2023, 2301316.

[S6] T. Zheng, M. Runowski, I.R. Martín, K. Soler-Carracedo, L. Peng, M. Skwierczyńska, M. Sójka, J. Barzowska, S. Mahlik, H. Hemmerich, F. Rivera-López, P. Kulpiński, V. Lavín, D. Alonso, D. Peng, *Adv. Mater.*, 2023, 2304140.

[S7] W. M. Piotrowski, R. Marin, M. Szymczak, E. M. Rodríguez, D.H. Ortgies, P. Rodríguez-Sevilla, M.D. Dramićanin, D. Jaque, L. Marciniak, *Adv. Opt. Mater.*, 2023, **11**, 2202366.

[S8] G. Guo, T. Yin, M. Dong, J. Nie, Y. Zhang, Z. Liu, F. Wang, X. Li, *Opt. Express*, 2023, **31**, 25978-25992.

[S9] B. Bai, P. Dang, D. Huang, H. Lian, J. Lin, *Inorg. Chem.*, 2020, **59**, 13481-13488.

[S10] C. Li, J. Zhong, *Chem. Mater.*, 2022, **34**, 8418.

[S11] T. Gao, W. Zhuang, R. Liu, Y. Liu, X. Chen, Y. Xue, *J. Alloys Compd.*, 2020, **848**, 156557.

[S12] G. Guo, T. Yin, M. Dong, J. Nie, Y. Zhang, Z. Liu, F. Wang, X. Li, *Opt. Express*, 2023, **31**, 25978-25992.

[S13] T. Yang, L. Chu, T. Zhang, Q. Zhou, Y. Qin, Z. Wang, J. Wan, M. Wu, *J. Alloys Compd.*, 2023, **965**, 171336.

[S14] J. Li, B. Liu, G. Liu, Q. Che, Y. Lu, Z. Liu, *J. Rare Earths.*, 2023, **41**, 1689.